Procedia Computer Science

Volume 80, 2016, Pages 1103–1113

ICCS 2016. The International Conference on Computational Science

Supersonic Airfoil Shape Optimization by Variable-Fidelity Models and Manifold Mapping

Jacob Siegler[1], Jie Ren[1], Leifur Leifsson[1,2], Slawomir Koziel[2], and Adrian Bekasiewicz[2]

[1]*Iowa State University, Ames, Iowa, USA*[*]

[2]*Reykjavik University, Reykjavik, Iceland*[†]

jsiegler@iastate.edu, jier@iastate.edu, leifur@iastate.edu, koziel@ru.is, bekasiewicz@ru.is

Abstract

Supersonic vehicles are an important type of potential transports. Analysis of these vehicles requires the use of accurate models, which are also computationally expensive, to capture the highly nonlinear physics. This paper presents results of numerical investigations of using physics-based surrogate models to design supersonic airfoil shapes. Variable-fidelity models are generated using inviscid computational fluid dynamics simulations and analytical models. By using response correction techniques, in particular, the manifold mapping technique, fast surrogate models are constructed. The effectiveness of the approach is investigated using lift-constrained drag minimization problems of supersonic airfoil shapes. Compared with direct optimization, the results show that an order of magnitude speed up can be obtained. Furthermore, we investigate the effectiveness of the variable-fidelity technique in terms of speed and design quality using several combinations of medium-fidelity and low-fidelity models.

Keywords: Supersonic airfoils, computational fluid dynamics, gradient-based search, adjoint sensitivity, surrogate-based optimization, variable-fidelity modeling, manifold mapping.

1 Introduction

Supersonic vehicles are currently being investigated as future civil transports. The analysis of these vehicles requires the use of accurate computational fluid dynamics (CFD) models to capture the highly nonlinear flow. Moreover, noise regulations for flight over land require aeroacoustic analysis of the entire vehicle shape. The models involved in the computational analyses are very expensive.

Surrogate models are widely used to create fast approximate models (Koziel *et al*., 2011). Surrogate modeling approaches can be roughly divided into two categories: (i) data-driven (or approximation-based) and (ii) physics-based. Data-driven surrogate models are constructed through approximations of the high-fidelity model data obtained in the process of sampling the design space using appropriate design of experiments (DOE) methodologies. Data-driven surrogates can be considered as generic

[*] Simulation-Driven Optimization Laboratory, Dept. of Aerospace Engineering, 537 Bissel Road, Ames, IA 50011, USA.

[†] Engineering Optimization & Modeling Center, School of Science and Eng., Menntavegur 1, 101 Reykjavik, Iceland.

Selection and peer-review under responsibility of the Scientific Programme Committee of ICCS 2016

doi:10.1016/j.procs.2016.05.416

models that are independent of the physics or any other knowledge about the problem at hand. The other class of models is based on exploitation of some knowledge about the system under consideration, usually embedded in physics-based low-fidelity models (Koziel *et al.*, 2011; Koziel and Leifsson, 2012).

In this work, we utilize physics-based surrogate-based optimization (SBO) techniques (Koziel *et al.*, 2011) for the design of supersonic aerodynamic surfaces at low computational cost. In particular, we use variable-fidelity models and a response correction technique, recently applied to aerodynamic shape optimization, namely, manifold mapping (MM) (Ren *et al.*, 2016), to construct fast surrogate models which are subsequently used within a SBO framework with trust regions. The approach is illustrated through lift-constrained drag minimization of supersonic airfoil shapes with 6 design variables. We investigate the effectiveness of the variable-fidelity techniques in terms of speed and design quality using combinations of medium-fidelity and low-fidelity models.

2 Computational Modeling of Supersonic Flow Past Airfoils

This section describes two modeling approaches for supersonic flow past airfoil shapes. The approaches are the shock expansion theory (low-fidelity), and computational fluid dynamics (CFD) analysis using governing equations for inviscid flow (medium-fidelity). CFD analysis using governing equations for viscous flow (high-fidelity) will be the subject of future work.

2.1 Shock Expansion Theory

The shock expansion model utilizes shock wave properties to solve pressure distribution around a supersonic airfoil by applying the Prandtl-Meyer functions. The procedure of obtaining coordinates to generate the biconvex airfoil is based on the geometry of a circle, illustrated below in Fig. 1. Assuming $c = 1$, where c represents chord length, the radius of the circle necessary to obtain a segment of desired z/c is found to be

$$r = \frac{\sqrt{0.5^2 + (z/2)^2}\,\sin\left(\frac{\pi}{2} - \arcsin\left(\frac{(z/2)}{\sqrt{0.5^2 + (z/2)^2}}\right)\right)}{\sin\left(\pi - 2\left(\frac{\pi}{2} - \arcsin\left(\frac{(z/2)}{\sqrt{0.5^2 + (z/2)^2}}\right)\right)\right)}, \tag{1}$$

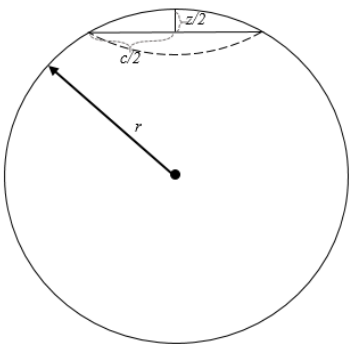

Figure 1: Geometric parameters for biconvex airfoil

where *z* represents the maximum thickness percentage of the airfoil. Once this radius is known, it can be used to find points around the airfoil, in particular the points above *c*, and assuming symmetry, the dotted curve below *c* as well.

In order to perform a successful shock expansion analysis, the airfoil must be broken down into a finite number of small segments, with length $ds_{i,k}$ on each segment, and for the case of the biconvex airfoil, equal turning angle $d\theta_{i,k}$, where *i* denotes the segment number and *k* the top or bottom of the airfoil. Fig. 2 gives relevant shape parameters of supersonic flow past a biconvex airfoil. The supersonic airfoil will encounter a shock wave, which forms at an angle β_k, measured as a positive angle from angle of attack α.

To start, the shock wave angle needs to be known. This allows us to solve for the Mach number downstream of the shock wave. This is obtained from

$$\cot\theta_{1,k} = \tan\beta_k \frac{(\gamma+1)M_\infty^2}{2\left(M_\infty^2 \sin^2\beta_k - 1\right) - 1}, \tag{2}$$

where γ is the heat capacity ratio, assumed to be 1.4. Rather than solving this equation for β_k, we utilize the Newton-Raphson technique,

$$u_{n+1} = u_n - \frac{f(u_n)}{f'(u_n)}, \tag{3}$$

to obtain a solution for β_k. The error criteria is set very low to ensure that an accurate shock wave angle is obtained, otherwise the rest of the calculations will be incorrect. Once β_k has been established, the downstream Mach $M_{1,k}$ can be found with

$$M_{1,k} = \sqrt{\frac{(\gamma-1)M_{\infty,k}^2 \sin^2\beta_k + 2}{\left(2\gamma M_{\infty,k}^2 \sin^2\beta_k - (\gamma-1)\right)\left(\sin^2\left(\beta_k - \theta_{1,k}\right)\right)}}, \tag{4}$$

where M_∞ represents the free-stream Mach number. Also, once the shock angle is known, the pressure relationship across the shock can be found as

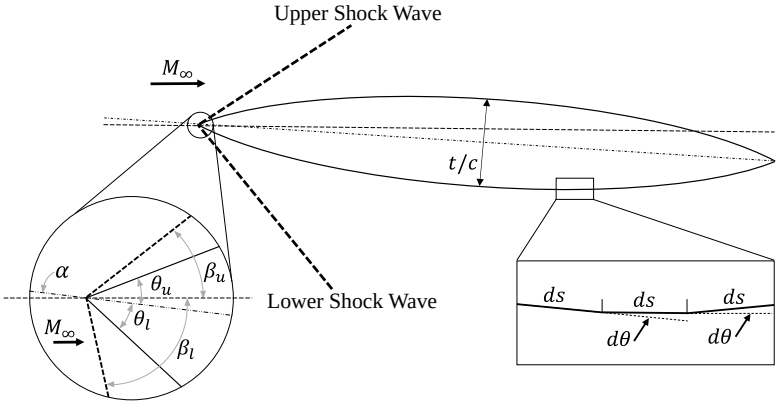

Figure 2: A schematic of supersonic flow past a biconvex airfoil indicating relevant parameters.

$$\frac{p_{1,k}}{p_\infty} = \frac{2\gamma M_{1,k}^2 \sin^2 \beta_k - (\gamma - 1)}{\gamma + 1}. \tag{5}$$

This can be stored as the first pressure relation back to the free-stream, and is needed to calculate the rest of the pressure distribution. Also, at this point, isentropic relations across the shock can be calculated. This includes the stagnation pressure relationship p/p_t and the Prandtl-Meyer angle ν. To continue the process along the airfoil, a new Prandtl-Meyer angle needs to be calculated simply by adding the change in deflection angle at the next consecutive panel with

$$\nu_{i,k} = \nu_{(i-1),k} + d\theta_{i,k}. \tag{6}$$

At this point, the Newton-Raphson method is called once more to solve for Mach number from

$$\nu_{i,k} = \sqrt{\frac{\gamma+1}{\gamma-1}} \arctan\left(\sqrt{\frac{\gamma-1}{\gamma+1}\left(M_{i,k}{}^2 - 1\right)}\right) - \arctan\left(\sqrt{M_{i,k}{}^2 - 1}\right). \tag{7}$$

This process is then repeated along the entire airfoil, storing each pressure relation along the way. Once these pressure relations have been calculated, they can be used to determine pressure coefficient at each panel from

$$\frac{p_{i,k}}{p_\infty} = \frac{p_{(i-1),k}}{p_\infty} \frac{p_{i,k}}{p_{t_{i,k}}} \frac{p_{t_{(i-1),k}}}{p_{(i-1),k}}, \tag{8}$$

and finally, to compute pressure coefficient, we use

$$C_{p_{i,k}} = \frac{2}{\gamma M_\infty^2}\left(\frac{p_{i,k}}{p_\infty} - 1\right). \tag{9}$$

Knowing the pressure distribution allows extra post processing of the data, such as obtaining the lift coefficient c_l and drag coefficient c_d. This is found by integrating the pressure about the airfoil surface. To model this integration, the summation of normal and axial force coefficients are found by

$$C_n = \sum_{k=1}^{2}\sum_{i=1}^{n} ds_{i,k} C_{p_{i,k}} \cos\theta_{i,k} \;,\; C_a = \sum_{k=1}^{2}\sum_{i=1}^{n} ds_{i,k} C_{p_{i,k}} \sin\theta_{i,k}, \tag{10}$$

and can finally be used to find lift and drag coefficients by converting to corresponding components with

$$C_l = C_n \cos\alpha - C_a \sin\alpha \;,\; C_d = C_n \sin\alpha + C_a \cos\alpha. \tag{11}$$

2.2 Inviscid CFD Model

The Stanford University Unstructured (SU^2) computer code is utilized for the inviscid fluid flow simulations. The steady compressible Euler equations are solved with an implicit density-based formulation. The convective fluxes are calculated using the second order Jameson-Schmidt-Turkel (JST) scheme. Three multi-grid levels are used for solution acceleration. Asymptotic convergence to a steady state solution is obtained in each case. The flow solver convergence criterion is the one that

occurs first of the two: (i) the change in the drag coefficient value over the last 100 iterations is less than 10^{-4}, or (ii) a maximum number of iterations of 1,000 is met.

An O-type computational mesh is generated using Pointwise (see Fig. 3). The farfield boundary is set 55 chord lengths away from the airfoil surface. The mesh density is controlled by the number of cells on the airfoil surface and the number of cells normal to the surface. The results of a grid convergence study, given in Table 1, revealed that a 512 × 512 mesh (shown number 5 in the table) is required for convergence within 0.1 drag count (1 drag count is $\Delta C_d = 10^{-4}$) when compared with the next mesh. Distance to the first grid point is 0.0004*c*. The flow simulation for Mesh 5 takes about 2.4 minutes. An adjoint solution for the drag coefficient take approximately the same amount of time. It should be noted that throughout an optimization run the airfoil shape may change significantly and the flow and adjoint simulation times may vary depending on the particular shape. For the optimization studies, Mesh 4 will be used as the medium-fidelity model **f**, and Mesh 1 as the low-fidelity model **c** (used only for manifold mapping). For the low-fidelity model, the maximum number of solver iterations is set to 300. The simulation time is less than 7 sec. Thus, the low-fidelity CFD model is about 20 times faster than the medium-fidelity model.

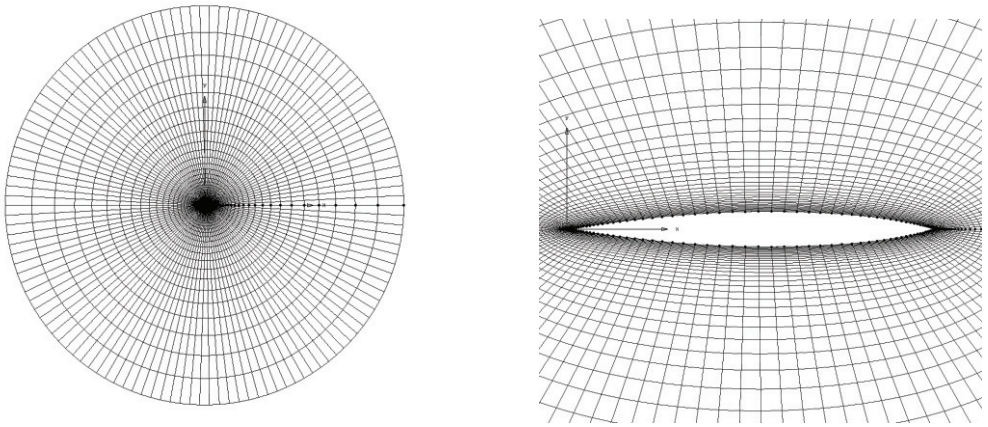

(a) (b)

Figure 3: An O-mesh used in the inviscid model: (a) farfield view, (b) a view close to the surface.

Table 1: Grid convergence study for the baseline airfoil shape using the inviscid CFD simulation model at a free-stream Mach number of $M = 2.0$ and an angle of attack $\alpha = 0.0°$.

Mesh	Grid Size	C_l	C_d	Simulation Time*
1	64 × 64 x 0.002	0.209288	0.050258	6.9 sec
2	128 × 128 x 0.001	0.209378	0.050279	19.4 sec
3	256 × 256 x 0.0006	0.209317	0.050256	58.7 sec
4	512 × 512 x 0.0004	0.209279	0.050241	2.4 min
5	1,024 × 1,024 x 0.0002	0.209332	0.050245	8.4 min

* Computed on a high-performance cluster with 32 processors. Flow solution only.

3 Supersonic Airfoil Shape Optimization

In this section, we describe the supersonic airfoil shape optimization. In particular, we describe the problem formulation, design variables, and the optimization techniques. Those include direct optimization using a gradient-based one with adjoint sensitivity information, and variable-fidelity optimization using manifold mapping.

3.1 Problem Formulation

The aerodynamic design problems considered in this work involve lift-constrained drag minimization of airfoils in two-dimensional flow where the simulations are performed using accurate, but computationally expensive, computational fluid dynamics (CFD) models, denoted by **f**. In general, nonlinear constrained optimization problems can be formulated as

$$\mathbf{x}^* = \arg\min_{\mathbf{x}} H(\mathbf{f}(\mathbf{x})) \text{ s.t. } \mathbf{g}(\mathbf{x}) \le 0, \mathbf{h}(\mathbf{x}) = 0, \ \mathbf{l} \le \mathbf{x} \le \mathbf{u}, \tag{12}$$

where $\mathbf{x}$ is the design variable vector of size $p \times 1$, $\mathbf{x}^*$ is the optimized design, H is a scalar valued objective function, $\mathbf{f}(\mathbf{x})$ is a vector of size $q \times 1$ with the figures of merit, $\mathbf{g}(\mathbf{x})$ is a vector of size $M \times 1$ with the inequality constraints, $\mathbf{h}(\mathbf{x})$ is a vector of size $N \times 1$ with the equality constraints, and $\mathbf{l}$ and $\mathbf{u}$ are the design variable lower and upper bounds, respectively, both vectors of the same size as $\mathbf{x}$. The vectors $\mathbf{f}(\mathbf{x})$, $\mathbf{g}(\mathbf{x})$, and $\mathbf{h}(\mathbf{x})$ are all obtained, or derived, from computationally expensive models.

In aerodynamic shape optimization, the high-fidelity model $\mathbf{f}$ calculates the figures of merit, e.g., in the two-dimensional case $\mathbf{f}$ can be composed as follows: $\mathbf{f}(\mathbf{x}) = [C_{l.f}(\mathbf{x}) \ C_{d.f}(\mathbf{x}) \ A(\mathbf{x})]^T$ where $C_{l.f}(\mathbf{x})$ is the nondimensional lift coefficient, $C_{d.f}(\mathbf{x})$ is the nondimensional drag coefficient, and $A(\mathbf{x})$ the airfoil cross-sectional area. The subscript f denotes the $\mathbf{f}$ model. In the case of a drag minimization problem, the objective function in (12) is set as $H(\mathbf{f}(\mathbf{x})) = C_{d.f}(\mathbf{x})$. The inequality constraint is set as $g_1(\mathbf{x}) = A_{min} - A(\mathbf{x}) \le 0$, where A_{min} is a minimum cross-sectional area, and $A(\mathbf{x})$ the cross-sectional area of the design $\mathbf{x}$. The equality constraint is $h_1(\mathbf{x}) = C_{l.t} - C_{l.f}(\mathbf{x}) = 0$, where $C_{l.t}$ is the target lift coefficient, and $C_{l.f}(\mathbf{x})$ is the lift coefficient of the current design. Here, the angle of attack, α, is used as a dummy variable to find the target lift coefficient value. All the constraints are handled directly in the optimization process.

3.2 Design Variables

The airfoil shape design variables are defined by the design variable vector $\mathbf{x}$. In this work, we write $\mathbf{x} = \mathbf{p}$, where $\mathbf{p}$ is a vector of size $m \times 1$, with m being the total number of control parameters of B-spline curves. The airfoil surfaces are written in parametric form as

$$x(t) = \sum_{i=1}^{n+1} X_i N_{i,k}(t), \ z(t) = \sum_{i=1}^{n+1} Z_i N_{i,k}(t), \tag{13}$$

where (x,z) are the Cartesian coordinates of the surface, $N_{i,k}$ is the B-spline basis function of order k, (X_i,Z_i) are the coordinates of the B-spline control polygon, and $n+1$ is the total number of control points. The control points are used as design variables and allowed only to move freely vertically as shown in Fig. 4 (the control points at the leading- and trailing-edges are fixed). Each designable control point is free to move in the vertical direction only. Thus, we have $\mathbf{x} = \mathbf{p} = [Z_1 \ Z_2 \ \ldots \ Z_{n+1}]^T$ and the corresponding X_i are fixed during the optimization. In this work, we use 3 free control points for each airfoil surface, i.e., there a total of 6 design variables.

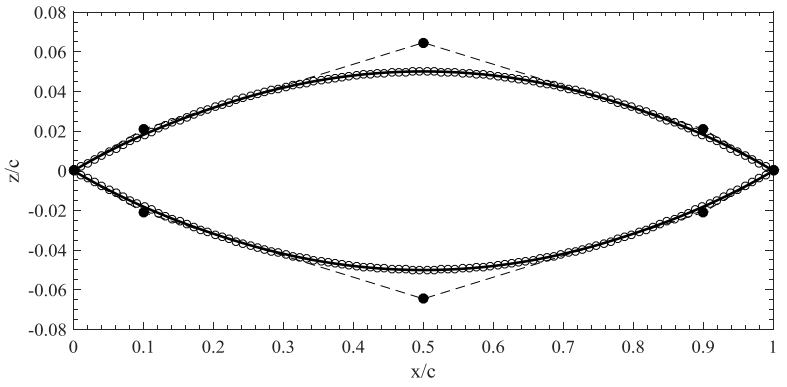

Figure 4: B-spline parameterization for the supersonic airfoil shape.

3.3 Direct Optimization

Direct optimization of the model **f** using a gradient-based algorithm exploiting adjoint sensitivities and trust regions is an iterative process

$$\mathbf{x}^{(i+1)} = \arg\min_{\mathbf{x}, \|\mathbf{x}-\mathbf{x}^{(i)}\| \le \delta^{(i)}} H(\mathbf{s}^{(i)}(\mathbf{x})), \tag{14}$$

where $\mathbf{x}^{(i)}$, i = 0, 1, …, is a sequence of approximate solutions to (12), whereas $\mathbf{s}_k^{(i)}(\mathbf{x})$ is a linear expansion of $\mathbf{f}(\mathbf{x})$ at $\mathbf{x}^{(i)}$ defined as

$$\mathbf{s}^{(i)}(\mathbf{x}) = \mathbf{f}(\mathbf{x}^{(i)}) + \nabla\mathbf{f}\ (\mathbf{x}^{(i)}) \cdot (\mathbf{x} - \mathbf{x}^{(i)}). \tag{15}$$

The gradient of the model **f** (applies separately for the drag and lift coefficient) is obtained by the adjoint equation. The linear model (15) satisfies the zero- and first-order consistency conditions with the function $\mathbf{s}^{(i)}(\mathbf{x})$ at $\mathbf{x}^{(i)}$, i.e., $\mathbf{s}^{(i)}(\mathbf{x}^{(i)}) = \mathbf{f}(\mathbf{x}^{(i)})$, and $\nabla\mathbf{s}^{(i)}(\mathbf{x}^{(i)}) = \nabla\mathbf{f}(\mathbf{x}^{(i)})$. Optimization of the linear model is constrained to the vicinity of the current design defined as $\|\mathbf{x} - \mathbf{x}^{(i)}\| \le \delta^{(i)}$, with the trust region radius $\delta^{(i)}$ adjusted adaptively using the standard trust region rules (Conn et al., 2000). The termination conditions for the algorithm (14) are: (i) $\|\mathbf{x}^{(i)} - \mathbf{x}^{(i-1)}\| < \varepsilon_x$, (ii) $|H^{(i)} - H^{(i-1)}| < \varepsilon_H$, (iii) $\delta^{(i)} < \varepsilon_\delta$, where ε_x, ε_H, and ε_δ are user defined convergence tolerances. For direct optimization of the aerodynamics design benchmark problems, we use: $\varepsilon_x = 10^{-6}$, $\varepsilon_H = 10^{-7}$, and $\varepsilon_\delta = 10^{-6}$. The solution of algorithm (14) with the model (15) is carried out using MATLAB's fmincon algorithm (MATLAB, 2015).

3.4 Variable-Fidelity Optimization by Manifold Mapping

A generic variable-fidelity optimization algorithm with trust regions produces a sequence $\mathbf{x}^{(i)}$, i = 0, 1, …, of approximate solutions to (12) using (14) with a surrogate model $\mathbf{s}^{(i)}(\mathbf{x})$ iteration i. The surrogate model **s** is a suitably corrected low-fidelity model **c**. In this work, we use manifold mapping (MM) (Echeverría-Ciaurri and Hemker, 2008; Ren *et al*., 2016).

In its basic version, the manifold mapping (MM) surrogate model is defined as (Ren *et al*., 2016)

$$\mathbf{s}^{(i)}(\mathbf{x}) = \mathbf{f}(\mathbf{x}^{(i)}) + \mathbf{S}^{(i)}\left(\mathbf{c}(\mathbf{x}) - \mathbf{c}(\mathbf{x}^{(i)})\right), \tag{16}$$

with $\mathbf{S}^{(i)}$ being the 3×3 correction matrix in our case (in general, the size of **S** is equal to the number of the components in **c**, **f**, and **s**)

$$\mathbf{S}^{(i)} = \Delta\mathbf{F} \cdot \Delta\mathbf{C}^{\dagger}, \tag{17}$$

where

$$\Delta\mathbf{F} = [\mathbf{f}(\mathbf{x}^{(i)}) - \mathbf{f}(\mathbf{x}^{(i-1)}) \quad \ldots \quad \mathbf{f}(\mathbf{x}^{(i)}) - \mathbf{f}(\mathbf{x}^{(\max\{i-n,0\})})], \tag{18}$$

and

$$\Delta\mathbf{C} = [\mathbf{c}(\mathbf{x}^{(i)}) - \mathbf{c}(\mathbf{x}^{(i-1)}) \quad \ldots \quad \mathbf{c}(\mathbf{x}^{(i)}) - \mathbf{c}(\mathbf{x}^{(\max\{i-n,0\})})]. \tag{19}$$

The pseudoinverse, denoted by †, is defined as

$$\Delta\mathbf{C}^{\dagger} = \mathbf{V}_{\Delta\mathbf{C}} \boldsymbol{\Sigma}_{\Delta\mathbf{C}}^{\dagger} \mathbf{U}_{\Delta\mathbf{C}}^{T}, \tag{20}$$

where $\mathbf{U}_{\Delta\mathbf{C}}$, $\sum_{\Delta\mathbf{C}}$, and $\mathbf{V}_{\Delta\mathbf{C}}$ are the factors in the singular value decomposition of the matrix $\Delta\mathbf{C}$. The matrix $\sum_{\Delta\mathbf{C}}{}^{\dagger}$ is the result of inverting the nonzero entries in $\sum_{\Delta\mathbf{C}}$, leaving the zeroes invariant.

The solution of algorithm (14) with the surrogate model (16) is carried out using the pattern search algorithm (Koziel, 2010), and the termination conditions are the same as for the direct optimization algorithm, but with $\varepsilon_x = 10^{-3}$, $\varepsilon_H = 10^{-4}$, and $\varepsilon_\delta = 10^{-3}$.

4 Numerical Investigation

We investigate the effectiveness of the variable-fidelity optimization technique when applied to the design of supersonic airfoil shapes. In particular, we compare supersonic airfoil shape optimization using MM with optimization using the conventional approach, i.e., gradient-based search with adjoint sensitivities. Moreover, we investigate how the fidelity of the lower fidelity model affects the optimization results, both in terms of optimization time as well as design quality.

4.1 Description of Design Problem

The objective is to minimize the drag coefficient (C_d) of the biconvex airfoil at a free-stream Mach number of $M_\infty = 2.0$, and a fixed lift coefficient $C_l = 0.22$. The task is to solve the following constrained optimization problem:

$$\min_{\mathbf{l} \le \mathbf{x} \le \mathbf{u}} C_d(\mathbf{x}), \tag{21}$$

subject to the following constraints

$$C_l(\mathbf{x}) = 0.22, \tag{22}$$

$$A(\mathbf{x}) \ge A_{baseline}, \tag{23}$$

where $A(\mathbf{x})$ is the cross-sectional area of the current design, and $A_{baseline}$ is the cross-sectional area of the baseline biconvex airfoil shape. The constant lift coefficient constraint is implicitly satisfied in the flow solver by using the angle of attack as a dummy parameter.

The B-spline parameterization approach, described in Sec. 3.2, is used for the upper and lower surfaces. We use 6 control points, as shown in Fig. 4, where two are fixed at the leading- and trailing-edges, and the other ones, 3 for each surface, can move in the vertical direction. This yields 6 design variables. Based on a fit to the biconvex, we set the x-locations of the free control points as: $\mathbf{X} = [\mathbf{X}_u; \mathbf{X}_l]^T = [0.1\ 0.5\ 0.9\ 0.1\ 0.5\ 0.9]^T$. The initial design variable vector is $\mathbf{x} = [\mathbf{x}_u; \mathbf{x}_l]^T = [0.0211\ 0.0646\ 0.0211\ -0.0211\ -0.0646\ -0.0211]^T$. The lower bound of $\mathbf{x}$ is set as $\mathbf{l} = [0\ 0\ 0\ -1\ -1\ -1]^T$, and the upper bound is set as $\mathbf{u} = [1\ 1\ 1\ 0\ 0\ 0]^T$.

The inviscid CFD model with a converged mesh (described in Section 2.2) is taken as the highest fidelity model **f**. The problem is solved using three approaches: gradient-based search using **f** and adjoints (described in Section 3.3), referred to here as Direct, manifold mapping (MM) (described in Section 3.4) with variable-resolution inviscid CFD models (here the low-fidelity model **c** is take as the coarsest mesh model described in Section 2.2), and MM with variable-fidelity physics models (here the low-fidelity model **c** is taken as the shock expansion model described in Section 2.1).

4.2 Results

Table 2 summarizes the results of the optimization runs. Figure 5 shows the convergence history of the algorithms. In particular, Fig. 5a shows the convergence of the argument **x**, and Fig. 5b shows the evolution of the drag coefficient in this case. All the algorithms terminate on the argument.

In terms of design quality, MM with variable-fidelity physics models obtained the lowest drag coefficient value of 493 counts. MM with variable-resolution models obtains a similar design (Fig. 6a). The direct algorithm did not make significant progress in optimizing the shape. In terms of the pressure coefficient distributions, shown in Fig. 6b, the shape obtained by multi-fidelity algorithms reduced the shock strength significantly when compared to the baseline pressure distribution. Figure 7 shows the Mach number contours for the baseline and the best optimized shape.

In terms of computational cost, the multi-fidelity algorithms need the least amount of simulations and wall-clock time. In particular, MM with variable-physics models needs 9 evaluations of **f** (N_f), and 647 evaluations of **c** (N_c); which, in total, is equivalent to less than 10 evaluations of **f** (N_{tot}). The total optimization time is about 25 minutes. MM with variable-resolution models needs to call **c** 123 times and **f** 2 times, which is equivalent to less than 21 evaluations of **f**. Direct needed 54 evaluations of **f** (includes both flow and adjoint solutions), and the total optimization time was about 326 min. Note that the multi-fidelity methods used in this study only require the flow solutions, but not the adjoint solutions like the gradient-based algorithm. Consequently, the MM algorithms are more efficient than the direct one for this particular case study. The variable-fidelity physics approach is significantly faster than the variable-resolution one due to a much faster lower fidelity model. The implementation of the variable-fidelity physics approach can be improved by having the lower fidelity model feed the higher fidelity one with information about the angle of attack needed to match the target lift coefficient (which is done in the variable-resolution approach). This should reduce the evaluations of **f** to one per iteration.

Table 2: Optimization results.

Parameter/Method	Baseline	Direct	MM with variable-resolution models	MM with variable-fidelity physics models
C_l (l.c.)	220.0	219.7	220.0	220.0
C_d (d.c.)	522.5	522.1	495.6	493.0
N_c	–	–	123	647
N_f	–	54*	2	9
N_{tot}	–	54*	< 21	< 10
t_c (min)	–	–	48.8	2.2
t_f (min)	–	325.7	5.2	22.6
t_{tot} (min)	–	325.7	54.0	24.8

* Primary flow solutions as well as adjoint solutions.

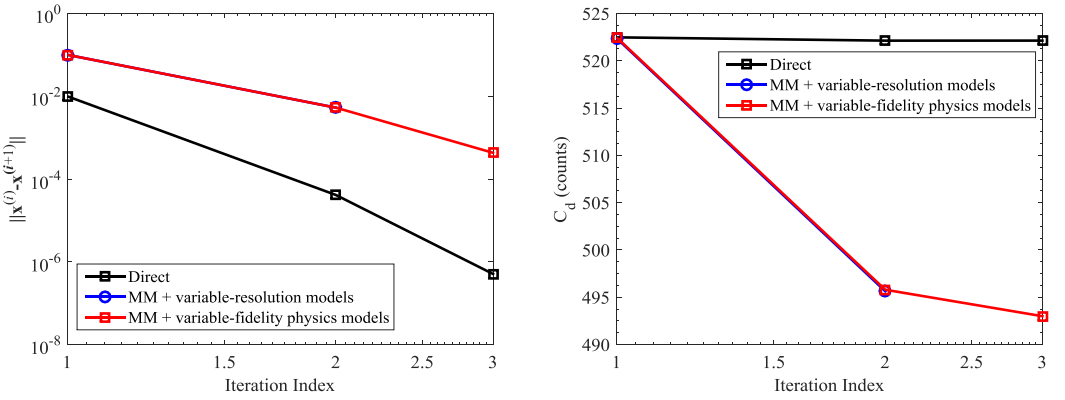

(a) (b)

Figure 5: Convergence histories of the optimization runs: (a) norm of the argument, and (b) evolution of the drag coefficient.

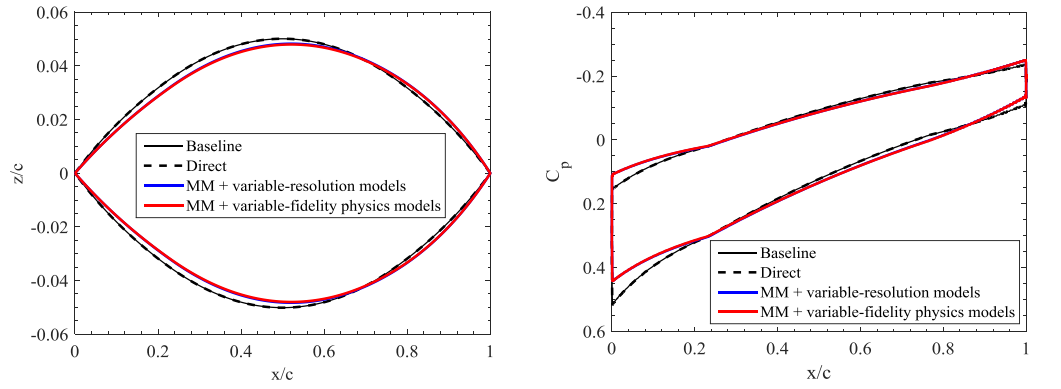

(a) (b)

Figure 6: Baseline and optimized characteristics: (a) shapes, (b) pressure coefficient distributions.

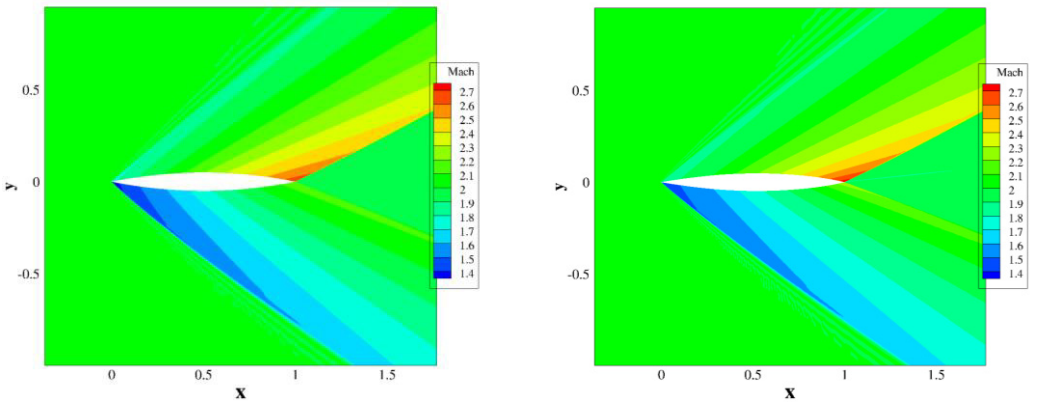

(a) (b)

Figure 7: Mach number contours at $M_\infty = 2.0$ and $C_l = 0.22$ for (a) the baseline, and (b) optimized shape with MM and variable-fidelity physics models.

5 Conclusion

A robust and computationally efficient optimization methodology for aerodynamic design of supersonic airfoils are presented. The approach uses low-fidelity models corrected by the response correction techniques (the manifold mapping method) to create fast and reliable surrogates which are utilized to search for approximate optimum designs of an expensive simulation model at a low CPU cost. The results of numerical investigations show that, when considering a low-dimensional problem, optimized designs are obtained at a significantly lower computational cost compared to direct gradient-based search with adjoint sensitivity information. Future work will consider higher fidelity computational models of supersonic flow past airfoils. In particular, we will use viscous flow simulations based on the Reynolds-averaged Navier-Stokes (RANS) equations and an appropriate turbulence model. This will significantly increase the computational cost compared to the inviscid model, by at least an order of magnitude. We will investigate using variable-fidelity physics modeling where we have the RANS model as the highest fidelity, and the inviscid and/or the shock expansion model as the lowest fidelity.

References

Bandler, J.W., Cheng, Q.S., Dakroury, S.A., Mohamed, A.S., Bakr, M.H., Madsen, K., Søndergaard, J. (2004) “Space mapping: the state of the art,” *IEEE Trans. Microwave Theory Tech*., 52, pp. 337−361.

Conn, A.R., Gould, N.I.M., and Toint, P.L., Trust Region Methods, MPS-SIAM Series on Optimization, 2000.

Echeverría-Ciaurri, D., and Hemker, P.W., “Manifold Mapping: a Two-Level Optimization Technique,” Computing and Visualization in Science, 11, pp. 193-206, 2008.

Koziel, S., “Multi-fidelity multi-grid design optimization of planar microwave structures with Sonnet,” International Review of Progress in Applied Computational Electromagnetics, Tampere, Finland, 2010, pp. 719-724.

Koziel, S., and Leifsson, L. (2012) Knowledge-based airfoil shape optimization using space mapping. *AIAA Applied Aerodynamics Conference*, New Orleans, Louisiana, June 25-28.

Koziel, S., Echeverría-Ciaurri, D., and Leifsson, L. (2011) “Surrogate-based methods,” in S. Koziel and X.S. Yang (Eds.) Computational Optimization, Methods and Algorithms, Series: Studies in Computational Intelligence, Springer-Verlag, pp. 33-60.

MATLAB V15.0, Mathworks Inc., Corporate Headquarters, 3 Apple Hill Drive, Natick, MA 01760-2098, USA.

Ren, J., Leifsson, L., Koziel, S., and Tesfahunegn, Y. (2016) “Multi-Fidelity Aerodynamic Shape Optimization Using Manifold Mapping,” *AIAA Aerospace Science and Technology Forum* (AIAA SciTech), San Diego, CA, Jan 4-8.